# High density single molecule surface patterning with colloidal epitaxy

Jerrod J. Schwartz and Stephen R. Quake[a)]
*Department of Bioengineering, Stanford University and Howard Hughes Medical Institute, Stanford, California 94305*

Simple and inexpensive methods for dense surface patterning of single molecules will help realize the massive potential throughput of molecular arrays in biology and nanoscience. To surpass the resolvable density limit imposed by random deposition, the authors have developed a method that uses colloids to pattern single molecules at a fixed length scale. They demonstrate the ability to pattern fluorescently labeled DNA such that ~38% of the available diffraction-limited regions contain exactly one molecule. This density is slightly less than the theoretical limit suggested by Monte Carlo simulations but surpasses the random deposition limit by more than threefold. © 2007 *American Institute of Physics.* [DOI: 10.1063/1.2772762]

With the application of spectroscopy to studies that require the interrogation of many molecules in parallel, there is growing interest in developing methods for strategically patterning different molecules on surfaces at small fixed length scales. A number of approaches have been developed to control the deposition of DNA molecules on surfaces, including molecular combing by capillary flow,[1] casting solutions on a surface prepatterned with polydimethylsiloxane (PDMS),[2] spin stretching,[3] and using a PDMS stamp inked with DNA for printing on mica.[4] Ordered DNA arrays have been generated by drop projection,[5] microcontact printing,[6] deposition on surfaces prepatterned by e-beam lithography,[7] and dip-pen nanolithography.[8] These approaches typically either yield high densities over small areas or low densities over large areas and are not well suited for single molecule deposition. Nanopatterning of DNA has been demonstrated on large surfaces of anodic porous alumina[9] and through the use of micron-sized beads to deposit nanoscale DNA spots,[10] but neither of these approaches has yet been demonstrated for single molecule deposition. Optical traps have been used to deposit single colloidal particles in a designed pattern,[11] but this approach has not yet scaled to deposit millions of features in a dense ordered array.

Optical resolution is traditionally determined by the Rayleigh criterion with the diffraction limited resolution defined by $d_R = 0.61\lambda/\text{NA}$, where $\lambda$ is the wavelength of collected photons and NA is the numerical aperture of the system. The theoretical density limit for single molecule surface patterning is the circle packing density limit: ~91% surface coverage and molecular spacing defined by $d_R$. There have been efforts to surpass the resolution limit using structured illumination patterns,[12] photoswitchable fluorophores,[13] and centroid localization methods[14] designed to resolve multiple single molecules within a diffraction limited region (DLR). While these techniques could conceivably be used to increase the maximum number of resolvable molecules while using a random deposition strategy, they may be difficult to scale up for large single molecule arrays.

Here, we demonstrate an approach to single molecule surface patterning that uses colloidal epitaxy to deposit individual double stranded DNA molecules with a minimum pitch of $d_R$. Briefly, silica colloids with diameter $d_R$ are functionalized with fluorescently labeled DNA; the colloids are self-assembled to form a monolayer on a coverslip using the DNA as a tether to the surface, and the colloids are subsequently removed to leave behind an ordered pattern of single DNA molecules. If the length of the tether between the colloid and the surface is small in comparison to the colloid diameter, this deposition strategy will theoretically allow every deposited single molecule to be spaced by at least a colloid diameter and be resolvable. An illustration outlining the colloidal epitaxy process is shown in Fig. 1.

We performed Monte Carlo simulations to determine the highest theoretical density achievable with a variety of patterning strategies, including colloidal epitaxy, random deposition, random deposition with image processing, and surface prepatterning methods. For the random deposition of molecules on a surface, we assigned $N$ molecules a random position on a continuous $XY$ grid containing $d$ DLRs. If $\delta = N/d$ is taken as the average number of deposited molecules per DLR and $\theta$ is the fraction of DLRs containing exactly one molecule, we found that $\theta$ reaches a maximum of
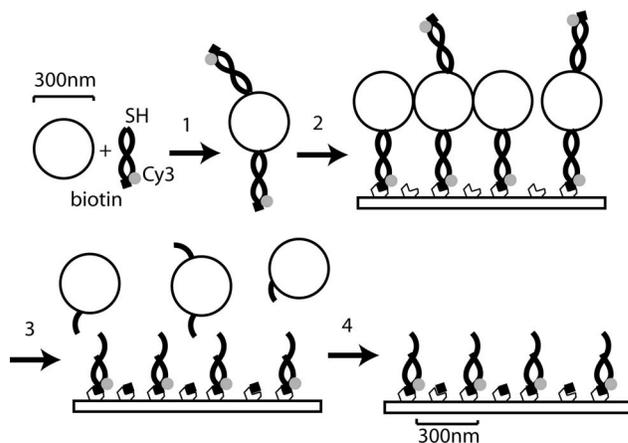


FIG. 1. Illustration of single molecule colloidal epitaxy (not to scale). (1) Aminated silica beads are coupled to thiolated double-stranded DNA decorated with Cy3 and biotin. (2) The DNA-bead conjugates are tethered to the surface through a biotin-neutravidin binding interaction. (3) Unoccupied neutravidin sites are filled with free biotin and the surface is incubated with a type II restriction enzyme to cleave the double-stranded DNA. (4) The beads are washed from the surface leaving behind an array of single molecules with a minimum pitch approximately equal to the colloid diameter.

[a)]Electronic mail: quake@stanford.edu

$\approx 0.12$ when $\delta = 0.37$. The relationship between $\theta$ and $\delta$ for this deposition approach is well described by the Poisson distribution $\theta(\delta) = \delta \exp(-\delta/0.32)$.

To see how image processing-based methods may improve feature density, we repeated the random deposition simulations while allowing molecules that shared a DLR with zero or one other molecule to be resolvable; any DLRs containing three or more resulted in all responsible molecules being flagged as unresolvable. With this approach, the fraction of DLRs containing resolvable single molecules improves to $\theta \approx 0.28$ when $\delta = 0.58$.

For the prepatterned surface simulations, molecules were only allowed to be immobilized on a rectangular array of features with a diameter of $\ll d_R$ and a pitch of $d_R$. Molecules deposited on different features are resolvable while two or more molecules on the same feature are unresolvable. In this case, the highest density occurs when $\delta = 1$, yielding a density of $\theta \approx 0.37$. Since this process contains defined features, the distribution follows Poisson statistics and the fraction of DLRs containing $m$ molecules is $\theta(\delta, m) = (\delta)^m e^{-\delta}/m!$. To find the conditions with the highest fraction of DLRs containing one molecule, we can take the derivative of $\theta$ with respect to $\delta$ and set it equal to zero, giving $d\theta/d\delta = e^{-\delta} - \delta^2 e^{-\delta} = 0$. The only non-negative solution to this equation occurs when $\delta = 1$. At this point the density reaches a maximum of $\theta = e^{-1} \approx 0.37$, which agrees with our simulations.

Single molecule colloidal epitaxy was implemented *in silico* by only permitting a molecule to be immobilized if its location was not located within the DLR of a molecule already on the surface. The density limit was found to be $\theta \approx 0.63$, which exceeds all other methods by nearly a factor of 2 and is approximately five times higher than can be achieved with random deposition. One can estimate the deposition time for colloidal epitaxy with the rate equation for the association/dissociation of DNA-colloid constructs, which takes the form

$$\frac{\partial C_s}{\partial t} = k_{on}(C_{s0} - C_s)C_w - k_{off}C_s, \qquad (1)$$

where $C_w$ is the concentration of the colloids in solution at time $t$, $C_0$ is the initial concentration of colloids before reaction, $C_s$ is the concentration of sites occupied, $C_{s0}$ is the total concentration of binding sites, and $k_{on}$ and $k_{off}$ are the rate constants for the association/dissociation events with units $M^{-1}\,s^{-1}$ and $s^{-1}$. Using the dimensionless parameters $\tau = Dt/h^2$ as the normalized diffusion time with $h$ as the height of the fluidic chamber and $D$ as the diffusion coefficient of the colloid, $\varepsilon = C_0/C_{s0}$ as the relative adsorption capacity of the surface with respect to the solution, $Da = k_{on}C_{s0}h^2/D$ as the Damköhler number, and $K_D = k_{off}/k_{on}C_0$ as the dissociation constant with concentrations $\theta_w = C_w/C_0$ and $\theta_s = C_s/C_{s0}$, Eq. (1) in dimensionless form is

$$\frac{\partial \theta_s}{\partial \tau} = \varepsilon Da[\theta_w(1 - \theta_s) - K_D\theta_s]. \qquad (2)$$

Solving this differential equation subject to the initial condition that $\theta(\tau = 0) = 0$ and neglecting any time dependence of $\theta_w$ gives the solution

$$\theta_s(\tau) = \frac{\theta_w}{\theta_w + K_D} - \frac{\theta_w}{\theta_w + K_D} \exp(-\varepsilon Da(\theta_w + K_D)\tau). \qquad (3)$$

Assuming that $K_D$ is small for a biotin-streptavidin binding interaction, Eq. (3) simplifies to

$$\theta_s(\tau) = 1 - \exp(-\varepsilon Da\theta_w\tau). \qquad (4)$$

The $k_{on}$ rate constant for streptavidin binding to biotinylated bovine serum albumin has been reported to be $1.2 \times 10^5 M^{-1}\,s^{-1}$.[15] Since this constant is directly proportional to the diffusion coefficients of the reacting species, we expect that biotin coupled to a 300 nm bead will reduce the rate constant by two orders of magnitude to $\sim 10^3 M^{-1}\,s^{-1}$. Using experimental values, one can then estimate that the time constant for deposition in Eq. (4) is $3 \times 10^{-6}\,s^{-1}$. This is in reasonable agreement with our experimental observations of 38% coverage after $\sim 40$ h of binding.

Double stranded DNA was coupled to 300 and 640 nm aminated silica colloids (corpuscular Inc.) as described elsewhere,[16] with stoichiometries experimentally determined such that the average number of DNA molecules per colloid was near unity [Fig. 1(a)]. The DNA sequence was designed to contain a Cy3 fluorophore, a BsaH I restriction site, a 5′-biotin, and a 3′-thiol (Integrated DNA Technologies, sequences 5′-Bio-CGC TCT ATC CTC CCT CCA TTC CAA CCA **GAC GCC** ACC CTC AGT CAT TTG TA-SH—3′ and 5′-TAC AAA TGA CTG AGG GT**G GCG TC**T GGT TGG AAT GGA GGG AGG ATA GAG CG -Cy3-3′, restriction site in bold). Imaging Cy3 with a 1.45 NA objective gives $d_R \approx 240$ nm; thus 300 nm colloids were chosen to ensure slightly more than adequate spacing. Glass coverslips (Precision Glass & Optics, D-263T cut glass, 0.15 mm, $2 \times 1$ in.$^2$ 40/20 surface quality) were RCA cleaned, coated with a polyelectrolyte multilayer, and functionalized with biotin-PEO-amine (Pierce), as previously described.[17] Surfaces were then washed with 1 mL of 10 mM Tris, 50 mM NaCl, pH 7.5 buffer, and incubated for 45 minutes with 1 mg/mL neutravidin (Pierce) in 0.01% sodium azide, 20 mM Tris, 100 mM NaCl, and pH 8 buffer. DNA-colloid constructs were resuspended in 100 $\mu$L of 1% BSA, 1X phosphate buffered saline (PBS), pH 7.4, and allowed to bind to the neutravidin surface for 20 h at 4 °C [Fig. 1(b)]. The surfaces were then washed with 1X PBS and the deposition process was repeated with a fresh batch of constructs. After the first deposition period of 20 h, the fraction of beads containing DNA in solution decreased slightly ($\sim 5\%$) due to deposition. Repeating the process serves two purposes: first, it allows us to verify and quantify the deposition; second, it helps to improve the deposition rate and surface density for the second incubation. After the final wash, unoccupied neutravidin sites on the surface were filled by incubation with 50 mM biotin for 30 min. The colloids were then removed with the addition of ten units of BsaH I in 1X buffer No. 4 (New England Biolabs) and 1% BSA for 2 h at 37 °C [Fig. 1(c)], followed by washing the surface extensively with de-ionized H$_2$O [Fig. 1(d)]. The surface was imaged on a Nikon TE2000-S microscope in total internal reflection fluorescence mode with a Hamamatsu ORCA-ER charged coupled device. A Cy3 filter set (HQ535/50, Q565LP, HQ610/75, Chroma) and a Nikon Plan Apo total internal reflection fluorescence (TIRF) 60$\times$ 1.45 NA objective with a low-fluorescence immersion oil was used ($n = 1.515$).
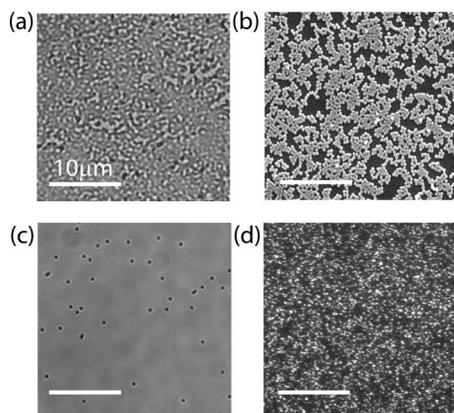
FIG. 2. Single molecule colloidal epitaxy in practice. (a) Bright field image of 300 nm beads immobilized on a neutravidin-coated glass coverslip through a biotinylated DNA tether. The image was taken in air after the colloid solution was removed with the surface still slightly wet. Drying was avoided primarily over concern that it would have undesirable effects on the DNA tether. (b) Scanning electron microscope image of 300 nm colloids tethered to the surface. (c) Bright field image of the surface following restriction enzymatic cleavage of the DNA tether and extensive washing. (d) Total internal reflection fluorescence image of Cy3-labeled DNA patterned on the surface after colloid removal. Scale bars are the same as in (a).

Figure 2 shows brightfield, scanning electron microscopy (SEM), and TIRF images of colloidal epitaxy using 300 nm silica colloids pre- and postenzymatic cleavage. Restriction enzyme treatment and washing was >90% successful at removing the colloids. Control experiments with non-biotinylated or nonthiolated DNA showed little nonspecific binding and DNA without Cy3 showed no sign of fluorescence. Images were processed using a custom script in MAT-LAB and single molecules were identified based on their fluorescent intensities and observing stepwise photobleaching in their trajectories. Figure 3(a) shows histograms of nearest-neighbor distances for Cy3 labeled DNA patterned with two colloid sizes, 300 and 640 nm, with peaks at 346 nm ($\sigma=48$ nm), and 641 nm ($\sigma=101$ nm), respectively. The average feature density of a 1 mm$^2$ field of view is shown in Fig. 3(b) and the mean experimental density was found to be 4.2 $\mu$m$^{-2}$ ($\sigma=0.3$ $\mu$m$^{-2}$), giving $\theta_s \approx 0.38$. Colloidal epitaxy thus allows for over a threefold improvement over random deposition, but the density is slightly lower than the $\sim$6.9 $\mu$m$^{-2}$ our simulations predicted possible.

We observed the colloid constructs forming quasihexagonal islands on the surface in the SEM images [Fig. 2(b)] and, to a lesser extent, in the fluorescence images [Fig. 2(d)]. The presence of these islands in both wet and dry states suggests that the colloids are likely forming these structures during convective assembly. This may be due to favorable colloid-colloid interactions during deposition or the nonuniform surface patterning of neutravidin, a phenomenon that has been previously observed.

Colloidal epitaxy may be used to pattern surfaces for many different single molecule studies. For example, DNA fragments with appropriate sticky ends may be ligated to the overhang created by the restriction digest for high throughput sequencing,[18] single nucleotide polymorphism genotyping, or enzymatic assays. This approach is not limited to depositing DNA on a surface: any molecule that can be heterofunctionalized with a reversible linker may be deposited, including small molecules, proteins, antibodies, viruses, or nanoparticles. Colloidal epitaxy relies on cheap and easily
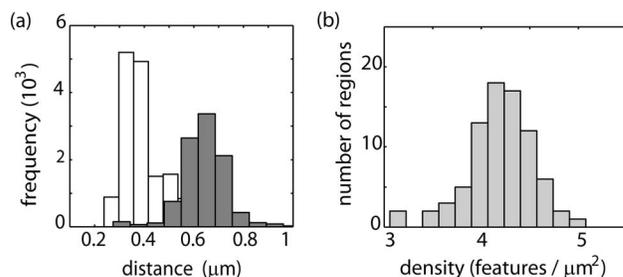


FIG. 3. (a) Nearest-neighbor intensity histogram for fluorophores deposited via colloidal epitaxy with 300 nm colloids (white) and 640 nm colloids (grey). The centroid of each single molecule feature was identified with single pixel precision and the linear distance to the next nearest feature was calculated in pixels. Pixel distances were then converted to nanometers based on known pixel dimensions. (b) Histogram of single molecule densities produced by 300 nm colloidal epitaxy observed in different fields of view over a 1 mm$^2$ area.

accessible reagents and does not require any expensive instruments, and the minimum spacing between molecules can easily be controlled by changing the colloid diameter. This gain in throughput may be of benefit to any study where many single molecules need to be interrogated in a massively parallel fashion.

[1] Z. Gueroui, C. Place, E. Freyssingeas, and B. Berge, Proc. Natl. Acad. Sci. U.S.A. **99**, 6005 (2002); Y. Y. Liu, P. Y. Wang, S. X. Dou, W. C. Wang, P. Xie, H. W. Yin, and X. D. Zhang, J. Chem. Phys. **121**, 4302 (2004).
[2] P. Bjork, A. Herland, I. G. Scheblykin, and O. Inganas, Nano Lett. **5**, 1948 (2005); D. Mijatovic, J. C. T. Eijkel, and A. van den Berg, Lab Chip **5**, 492 (2005).
[3] H. Yokota, J. Sunwoo, M. Sarikaya, G. van den Engh, and R. Aebersold, Anal. Chem. **71**, 4418 (1999).
[4] H. Nakao, M. Gad, S. Sugiyama, K. Otobe, and T. Ohtani, J. Am. Chem. Soc. **125**, 7162 (2003).
[5] V. Dugas, J. Broutin, and E. Souteyrand, Langmuir **21**, 9130 (2005); M. Fujita, W. Mizutani, M. Gad, H. Shigekawa, and H. Tokumoto, Ultramicroscopy **91**, 281 (2002).
[6] S. A. Lange, V. Benes, D. P. Kern, J. K. H. Horber, and A. Bernard, Anal. Chem. **76**, 1641 (2004).
[7] G. J. Zhang, T. Tanii, T. Funatsu, and I. Ohdomari, Chem. Commun. (Cambridge) **2004**, 786.
[8] L. M. Demers, D. S. Ginger, S. J. Park, Z. Li, S. W. Chung, and C. A. Mirkin, Science **296**, 1836 (2002); N. L. Rosi and C. A. Mirkin, Chem. Rev. (Washington, D.C.) **105**, 1547 (2005).
[9] F. Matsumoto, M. Kamiyama, K. Nishio, and H. Masuda, Jpn. J. Appl. Phys., Part 2 **44**, L355 (2005).
[10] P. Pammer, R. Schlapak, M. Sonnleitner, A. Ebner, R. Zhu, P. Hinterdorfer, O. Hoglinger, H. Schindler, and S. Howorka, Chem. Phys. Chem. **6**, 900 (2005).
[11] J. P. Hoogenboom, Appl. Phys. Lett. **80**, 4828 (2002).
[12] M. G. L. Gustafsson, Proc. Natl. Acad. Sci. U.S.A. **102**, 13081 (2005).
[13] M. J. Rust, Nat. Methods **3**, 793 (2006).
[14] M. P. Gordon, T. Ha, and P. R. Selvin, Proc. Natl. Acad. Sci. U.S.A. **101**, 6462 (2004); X. H. Qu, D. Wu, L. Mets, and N. F. Scherer, ibid. **101**, 11298 (2004); A. Yildiz, J. N. Forkey, S. A. McKinney, T. Ha, Y. E. Goldman, and P. R. Selvin, Science **300**, 2061 (2003).
[15] T. Gervais, Chem. Eng. Sci. **61**, 1102 (2006).
[16] M. Hegner, Single Mol. **1**, 139 (2000).
[17] E. P. Kartalov, M. A. Unger, and S. R. Quake, BioTechniques **34**, 505 (2003).
[18] I. Braslavsky, B. Hebert, E. Kartalov, and S. R. Quake, Proc. Natl. Acad. Sci. U.S.A. **100**, 3960 (2003).